

Neutron Flux Measurement in TRIGA Reactor using Gold Foil Activation Method

Tornike Kimeridze^{1,2}; Tran Canh Hai Nguyen³

¹ LEPL - David Aghmashenebeli National Defence Academy of Georgia

² LEPL - Ilia Vekua Sukhumi Institute of Physics and Technology

³ Dalat Nuclear Research Institute, Dalat, Vietnam

Abstract

Neutron flux measurement is integral to nuclear physics, with implications across nuclear engineering, medical physics, and material science. This study details neutron flux mapping in the TRIGA reactor in Vienna using the gold foil activation method. Identical gold foils were prepared, subjected to 10-minute irradiation within the reactor core, and subsequently assessed using a $4\pi\beta$ counter. The neutron flux distribution was theoretically modeled as a Bessel function and cross-referenced against measured activities to yield an experimental thermal neutron flux map. Findings reveal a close alignment between theoretical and experimental data, with a slight flux increase at the core's outermost periphery due to the graphite reflector. This work contributes valuable data on the TRIGA reactor's neutron flux distribution, with broader applicability in the field of reactor experiments and operation.

Keywords: Neutron flux; Activation analysis; Experimental nuclear physics, Reactor physics.

1. Introduction

Determining the neutron flux is essential for both ensuring the safety and efficiency of nuclear reactors and for designing new ones, as it impacts the rate of neutron-induced processes like fission and activation. To measure this, the gold foil activation method is often employed; it involves irradiating gold foils at different distances from the reactor core and then measuring the induced radioactivity to determine the flux. This technique is widely recognized, has had a long history, and is frequently used in dosimetry for reactors [1].

This paper presents a study that employed the gold foil activation method to quantify thermal neutron flux in Vienna's TRIGA reactor. The TRIGA reactor, designed for safety and operational ease, serves a diverse range of functions including educational training in reactor physics, R&D in areas like material

science and neutron imaging, isotope production for medical and industrial use, research in radiation therapy techniques, and testing of nuclear safeguards approach for international compliance [2, 3, 4]. Its versatility also extends to environmental studies, where it is used for neutron activation analysis to identify trace elements and determine the age of samples.

The primary objective is to offer a precise and detailed experimental protocol for measuring thermal neutron flux, designed to minimize errors while thoroughly elucidating the theoretical foundations and rationale for each step in the procedure.

2. Theoretical background

The study took place at Vienna's Atominstitut, which houses Austria's only reactor [3]. This TRIGA reactor is a multipurpose pool-type reactor. It utilizes UZrH fuel and is outfitted with graphite reflectors. Operating at a maximum thermal neutron flux density of 1×10^{13} n/cm² · s and a power output of 250 kW, the reactor features a built-in safety mechanism: its fuel material and structure exhibit a negative temperature coefficient, causing the reactor power to decrease automatically if the fuel temperature rises beyond a certain threshold. The core is comprised of 83 fuel rods and is encased in a graphite reflector.

Neutron flux can be categorized into three groups according to their energy spectrum [5]:

- Thermal neutrons: 0 – 0.1 eV, with Maxwell's equations.
- Epithermal neutrons: 0.1 eV – 1 MeV, with $1/v$ ($1/E$) distribution.
- Fast neutrons: 1 – 10 MeV, with Watts' distribution.

In nuclear reactors, thermal neutron flux is pivotal for multiple key aspects including power output, fuel burnup, and safety. It directly affects the rate of fission, the main process for energy generation. A stable thermal neutron flux is indispensable for operational safety and efficiency, influencing reactor control and diagnostics. It is also critical for material testing, isotope production, and research. Accurate measurement, such as through the gold foil activation technique, is essential for calibrating safety systems, optimizing fuel use, and developing new reactor designs.

To establish an accurate relationship between measured activity and actual neutron flux, it is necessary to account for various correction factors [13] such as the cadmium correction factor, neutron self-shielding factor, β self-shielding factor, Wescott factor, and detector efficiency. Additionally, parameters like the activation cross-section, irradiation time, and decay time are critical to the analysis. Each of these factors and factors is delineated in the subsequent subsections, beginning with an examination of the theoretical thermal flux shape.

2.1. Neutron flux distribution for pool-type reactor

One-group time-dependent neutron diffusion equation for a homogenous reactor, bare reactor is

$$D\nabla^2\Phi - \Sigma_a\Phi + s = -\frac{1}{v}\frac{\partial\Phi}{\partial t} \quad (1)$$

The balance between source, absorption and neutron leakage always exists (the right-hand side term of equation (1) is eliminated). To ensure this balance, we multiply the source term by a factor of $1/k$, k being an unknown constant.

$$D\nabla^2\Phi - \Sigma_a\Phi + \frac{1}{k}v\Sigma_f\Phi = 0 \quad (2)$$

Given that $B_g^2 = \frac{1}{D}\left(\frac{1}{k}\Sigma_f - \Sigma_a\right)$ is geometrical buckling, equation (2) becomes:

$$\nabla^2\Phi + B_g^2\Phi = 0 \quad (3)$$

The solution of equation (1) for a finite cylinder of height H and radius R , the flux depends on the distance r from the axis and the distance z from the midpoint of the cylinder is

$$\Phi(\vec{r}) = R(r)Z(z) \quad (4)$$

With

$$Z_m(z) = A_m \cos\left(\frac{m \cdot z \cdot \pi}{H}\right) \quad (5)$$

$$R_n(r) = A_n J_0\left(\frac{x_n r}{R}\right) \quad (6)$$

Therefore, the neutron flux density distribution is:

$$\Phi(\vec{r}) = \Phi_0 \cdot J_0\left(\frac{2.405r}{R}\right) \cos\left(\frac{\pi \cdot z}{H}\right) \quad (7)$$

where:

H (cm) – extrapolated height of the active core.

R (cm) – extrapolated radius of the active core.

J_0 – Bessel function of first kind of order zero.

Φ_0 – first null solution of J_0 .

x_n – n^{th} null solution of J_0 .

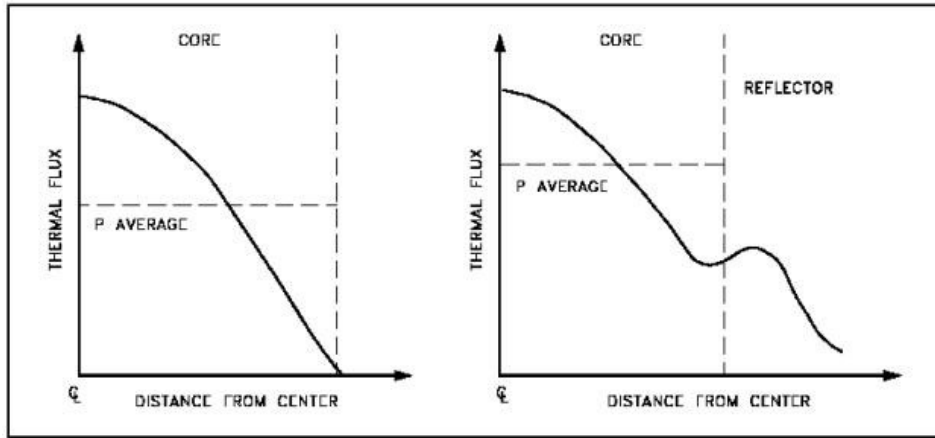


Figure 1. Radial shape of thermal neutron flux [6]

2.2. Neutron flux determination using the gold foil activation method

The gold foil activation technique is based on the concept that a neutron interacting with an ^{197}Au nucleus may be absorbed, thereby creating an unstable ^{198}Au isotope. This isotope subsequently decays into ^{198}Hg , emitting β particles and γ rays in the process. By quantifying the activity of the resulting ^{198}Hg , the neutron flux can be determined. This neutron activation and decay process is outlined as follows:

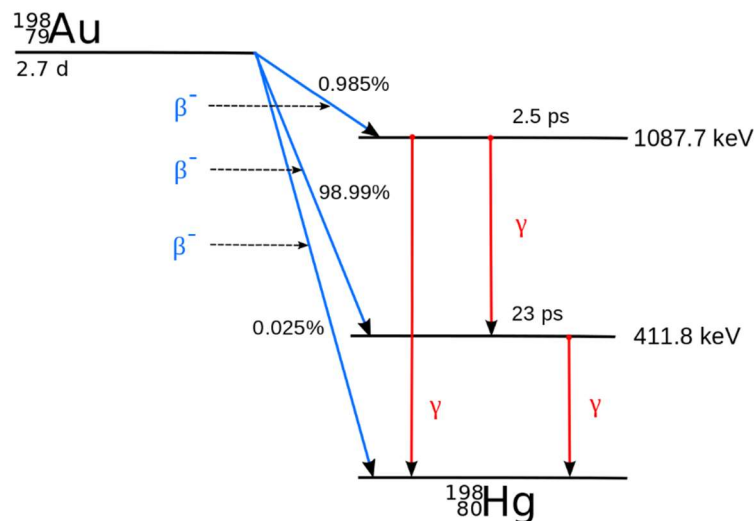
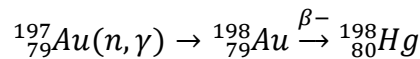


Figure 2. Decay scheme of ^{198}Au [7].

The ideal foil for flux measurement should have a simple decay scheme for accurate absolute counting, a well-known activation cross-section that closely adheres to the $1/v$ law, and a conveniently long half-life. Among available probe materials—such as ^{47}In , ^{25}Mn -25, ^{27}Co -27, and ^{47}Ag -47—gold is the standard [4]. It has a well-characterized activation cross-section at a neutron speed of $v_0 = 2200 \text{ m/sec}$ ($\sigma_{act} = 98.5 \pm 0.4 \text{ barn}$), a g-factor (Westcott factor) consistently close to one, and a half-life that is

sufficiently long (2.7 days) for taking measurements. Its simple decay scheme, shown in Figure 2, also facilitates precise absolute counting. Other advantages of using gold include its mechanical flexibility, owing to the absence of a crystal structure, and its relatively low cost at high purity levels (approximately 100%).

Aluminum was used as the sample holder due to its short half-life (~7 min), small neutron absorption cross-section ($\sigma_a = 0.231 \text{ barn}$), low density ($\rho = 2.7 \text{ g/cm}^3$), and mechanical integrity in highly radioactive conditions [8].

Once the foils are irradiated and their activities determined, we need to correlate that activation of different foils to the neutron flux at that location. To accomplish this, we need to define some fundamental concepts.

Activity

Activation rate C refers to the quantity of radioactive atoms generated per second per cm^2 of foil surface due to neutron capture. In the context of thin foils, this activation rate is directly proportional to either the neutron flux or the density of the material. When focusing on thermal neutron flux, the activation cross-section adheres to the $1/v$ law, as dictated by the Maxwell-Boltzmann distribution. Consequently, it is possible to determine the neutron flux based solely on the activation rate, without requiring knowledge of the neutron spectrum. C is described by

$$C = \Phi \bar{\Sigma}_{act} d \quad (8)$$

Where Φ ($\text{n/cm}^2 \cdot \text{s}$) is the thermal neutron flux, $\bar{\Sigma}_{act}$ (barn) is the activation cross section and d (cm) is foil thickness.

The total activation represents the number of radioactive atoms per cm^{-1} of foil area at any given time. For a constant activation rate starting at $t = 0$, $B(t)$ is expressed by the equation:

$$B(t) = \frac{C}{\lambda} (1 - e^{-\lambda t}) \quad (9)$$

Here, λ (s^{-1}) is the decay constant at $t = 0$. Upon “infinitely long” irradiation, $B(t)$ approaches the saturation value C/λ .

After irradiation ceases, $B(t)$ falls off according to the law:

$$B(t_2) = \frac{C}{\lambda} (1 - e^{-\lambda t_1}) e^{-\lambda t_2} \quad (10)$$

Where t_1 is the duration of the irradiation period and t_2 is the time elapse after the end of irradiation.

Activity A is the number of atoms decaying per sec and cm^2 of the surface. Here we should distinguish between theoretical activity A_t and experimental activity A_e . $A_t = \lambda B$ (11) and $A_t(t_2) = C(1 - e^{-\lambda t_1}) e^{-\lambda t_2}$ (12) or

$$A_t T = C \quad (13)$$

With the time factor being

$$T = \frac{e^{\lambda t_2}}{1 - e^{-\lambda t_1}} \quad (14)$$

The activity experimentally measured by the gas flow counter is related to the theoretical activity first by

$$A_e = \varepsilon \cdot F \cdot A_t \quad (15)$$

Where F is foil area, and ε is counter efficiency.

Self-shielding factor G_{th}

Due to the non-negligible thickness of the gold foil, some neutrons will be absorbed within the material. This lead to a lower average thermal neutron flux within the foil, denoted as $\bar{\Phi}_{th,sample}$, compared to the average thermal neutron flux at the foil's surface, $\bar{\Phi}_{th}$. The ratio between these two flux values is referred to as the self-shielding factor:

$$G_{th} = \frac{\bar{\Phi}_{th,sample}}{\bar{\Phi}_{th}} \quad (16)$$

Activation cross section of thermal neutrons

At conditions of room temperature, $T_0 = 293 \text{ K}$ (20°C) and $E_0 = k \cdot T = 0.0025 \text{ eV}$, the following relationship between neutron cross section at neutron temperature T_n and at T_0 can be derived from Westcott formalism as follows:

$$\sigma_{\bar{v},act}(T_n) = \sigma_{0,act} \frac{\sqrt{\pi}}{2} \sqrt{\frac{T_0}{T_n}} \quad (17)$$

β self-absorption

It is not advisable to use foils thicker than those corresponding to maximum sensitivity for flux measurement. The sensitivity of the foil diminishes with increased thickness because, in beta-counting, only a thin surface layer effectively contributes to the measurement. As foil thickness increases, the likelihood of neutrons penetrating this effective region from deeper layers decreases, while the probability of backscatter processes increases. Therefore, it's crucial to use the thinnest foil material feasible for accurate measurements.

β self-absorption can be approximated using an exponential law of attenuation: For a β -emitter with a negligibly small surface area covered by a layer of thickness x , the probability $w(x)$ that a decay β particle penetrates the layer is given by

$$w(x) = e^{-\alpha x} \quad (18)$$

Therefore, the expression for β self-absorption can be written as follows [9]:

$$\varepsilon_{\beta} = \frac{\int_0^{\theta} e^{-dx} dx}{\theta} = \frac{1 - e^{-\mu\theta}}{\mu\theta} \quad (19)$$

where μ ($cm^2 \cdot g^{-1}$) is absorption coefficient of the foil for β ; and θ ($g \cdot cm^{-2}$) is foil thickness.

Sensitivity of the counter

To ascertain the sensitivity ε of the counter, two measurements are conducted using the same foil and counter. The first measurement is taken with the foil deposited on the counter's sample holder, resulting in a sensitivity value of ε_1 . For the second measurement, the foil is covered on top with an additional sample holder, producing a sensitivity value labeled ε_2 .

$$\varepsilon = \frac{\varepsilon_1}{\varepsilon_2} \quad (20)$$

Cd-cover method and Cd correction factor

The presence of epithermal neutron flux and the gold foil's notable activation cross-section for these neutrons result in significant epithermal activity. To isolate this from the total activity, cadmium (Cd) is employed. Cd's large absorption cross-section for thermal neutrons effectively screens them, while allowing epithermal neutrons with energies above 0.4 to 0.7 eV to interact with the gold, depending on the Cd layer thickness.

To quantify thermal neutron-induced activity, two identical foils—one bare and one Cd-covered—are irradiated simultaneously. By comparing their resulting activities, the thermal and epithermal contributions can be differentiated.

It's important to note that the Cd "cut-off" energy does not strictly match the upper energy limit of thermal neutrons but also includes some epithermal ones. Thus, a Cd-correction factor is introduced to ensure accurate representation of solely the thermal neutron flux in the activity difference between the two foils.

$$A_{th} = A_b - A_{Cd} \quad (21)$$

In which A_{th} is the activity from thermal neutrons; A_b is the activity from bare gold foil; and A_{Cd} is activity from Cd-covered gold foil.

Cd-correction factor is defined as

$$F_{Cd} = \frac{A_b}{A_{Cd}} = \frac{A_{th} - A_{epi}}{A_{epi}} = 1 + \frac{A_{th}}{A_{epi}} \quad (22)$$

Following the process outlined above, thermal activation as a function of foil thickness, neutron flux, activation coefficient and absorption coefficient is expressed as

$$C_{th} = \mu_{act} \delta \frac{\varphi_0(\mu_{act} \delta)}{2\mu_{act} \delta} \Phi_{th} \quad (23)$$

For thin foils $\mu_{act} \delta \ll 1$ at pure 1/v absorber, Westcott coefficient $g = 1$ and resonance integral $s = 0$, we have

$$\Phi_{th} = \frac{2A_{th}T}{\sqrt{\pi} \sqrt{\frac{T_0}{T_n}} (\mu_{act}(v_0)\delta)} \quad (24)$$

With activation and absorption coefficients ratio

$$\frac{\mu_{act}}{\mu_a} = S_\beta \cdot G \quad (25)$$

Where S_β is the β self-absorption coefficient; and G being the neutron self-shielding coefficient of gold.

Here we arrive at the complete equation to determine thermal neutron flux considering all attendant factors is:

$$\Phi_{th} = \frac{2(1 - e^{-\lambda t_1})}{\varepsilon \cdot F \cdot S_\beta \cdot \delta \cdot G \cdot \mu_a \cdot \sqrt{\pi} \sqrt{\frac{T_n}{T_0}}} [A_t e^{\lambda t_2} - F_{cd} \cdot A_{cd} e^{\lambda t_2'}] \quad (26)$$

Specifications of the gold foils and the values of relevant factors are:

$\alpha = 1$ (isotope enrichment)

$\delta = \frac{m_b}{F}$ (mass surface loading)

$m_b = 0.0079$ (g) (gold foil mass)

$F =$ diameter of gold foil

$R = 0.32$ (efficiency for 2π – detector) [10]

$\frac{T_N}{T_0} = 1.07$ [4]

$t_1 = 10$ minutes (activation time)

$\lambda = \frac{\ln 2}{T_{1/2}} = 1.783 \times 10^{-4}$ min (decay constant)

$t_2 = 60$ hour (decay time for bare foil)

$t_2' = 65$ min (decay time for covered foil)

$$F_{cd} = 1.22 \text{ (cadmium correction factor) [11]}$$

$$G_{th} = 0.9766 \text{ (self – shielding factor) [4]}$$

$$S = 0.6968 \text{ (beta self-absorption) [4]}$$

3. Experiment setup

3.1. Measurement locations

The neutron flux measurement using the gold foil activation method was conducted by irradiating gold foils at separate positions on the same axis on the azimuthal plane to cover radial neutron flux distribution of the reactor from the center of the core to the periphery.

A picture of core map is shown in Figure 2, left side view, while the corresponding positions of fuel rods and irradiation channels are illustrated by the schematic on the right. The exact distances between each irradiation channel can be found in Table 1, with the insertion of samples done at channels b, f, i, l, and o.

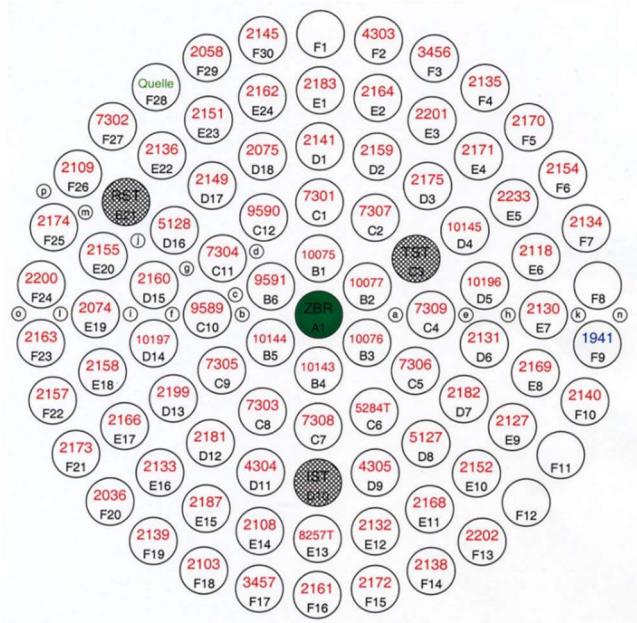
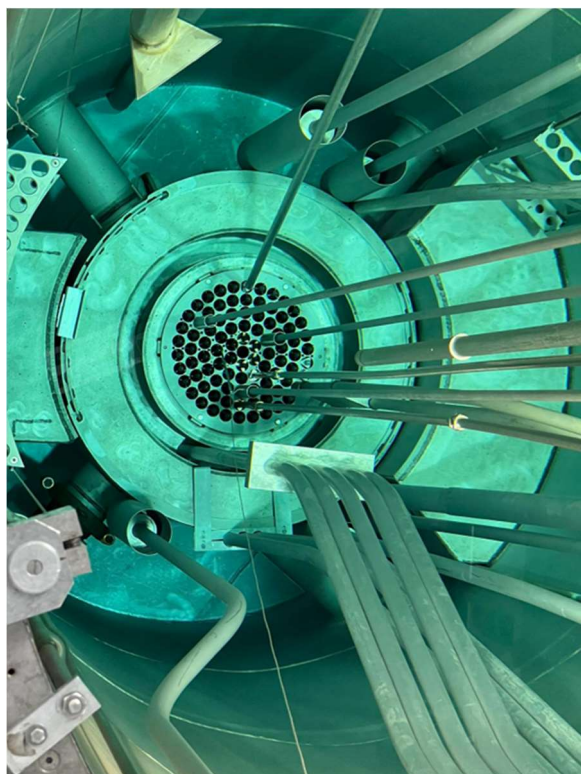


Figure 3. TRIGA core (left) and core map (right)

It should be noted that the locations of the foils were carefully selected to be away from any control rods, to avoid flux depression caused by neutron capture.

Table 1. Positions of experimental holes in reactor core

Position	Distance (cm)
a, b	5,3
d	6,0
c	6,2
g	9,7
e, f	10,6
h, i	13,5
j	13,8
m	17,6
k, l	18,5
n, p, o	21,3
Diameter of an irradiation hole	7,95 mm

3.2. Experiment procedure

In nuclear physics experiments, careful preparation of samples and proper calibration of measuring instruments, including activity counters, scales and detectors, are essential for accurate and reliable measurements.

The samples used in the experiment involve Cd sheaths with a thickness of 0.5 mm, Au foils with a weight spread of 40 mg/cm² and a diameter of 5 mm. In terms of measuring device, an analytical scale with an accuracy of 0.0001 g and a $4\pi\beta$ counter are used.

3.2.1. Equipment for measurement

For absolute activity measurement, the standard is the $4\pi\beta$ - γ coincidence counter. However, this approach has limitations such as difficulty in detecting low activities and stringent setup requirements. These include no electron conversion, positional-independence of sensitivity, and counter specificity to the radiation type being measured. Therefore, we opted for a $4\pi\beta$ flow-type proportional counter, simplifying the apparatus while still accomplishing the objective [9].

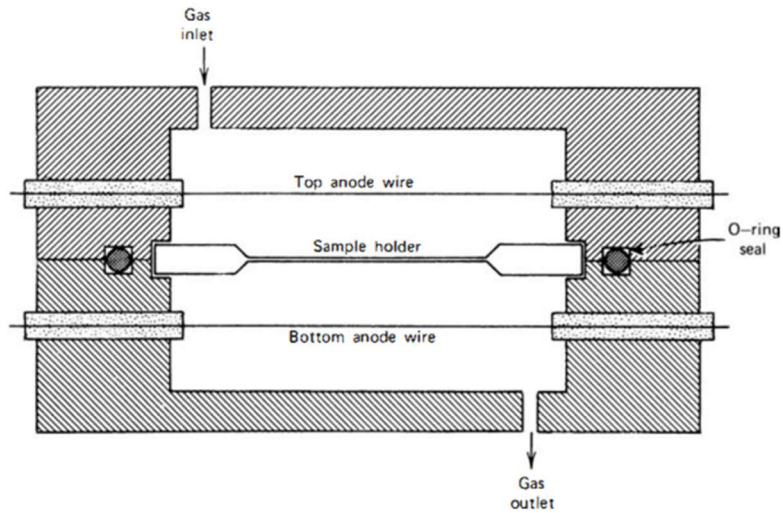


Figure 4. Schematic of a 4π gas flow proportional counter [14]

3.2.2. Samples preparation

To standardize the samples, individual gold foils are cut to achieve uniform shape and size. These foils are weighed on a high-precision electronic scale and cleansed with alcohol to remove contaminants and any adhering organic substances. The foils are subsequently positioned in sample holders and secured with tape. One foil in each holder is shielded with Cd, while its counterpart remains unshielded. A total of five sample holders are utilized, each containing two gold foils.



Figure 5. Aluminum sample holder (bottom) and experimental equipment (top)



Figure 6. Gold foils (left) and cleaning alcohol (right)

3.2.3. Irradiation of samples

To initiate sample irradiation, the reactor is stabilized at 10 Watts for a 20-second period, accounting for foil activation during start-up. Samples are then accurately positioned in the core and irradiated for 10 minutes. Post-irradiation, the reactor is deactivated, and samples are removed and allowed to decay until their activity reaches background levels, ensuring that ^{27}Al activity becomes negligible to minimize error.



Figure 7. Inserting sample holders into the reactor core

3.2.4. Activity measurement

Upon removal, foils are meticulously flattened to preserve their surface area for accurate activity counting. They are systematically grouped to enable precise radial distribution analysis, facilitating the assessment of neutron flux distribution.

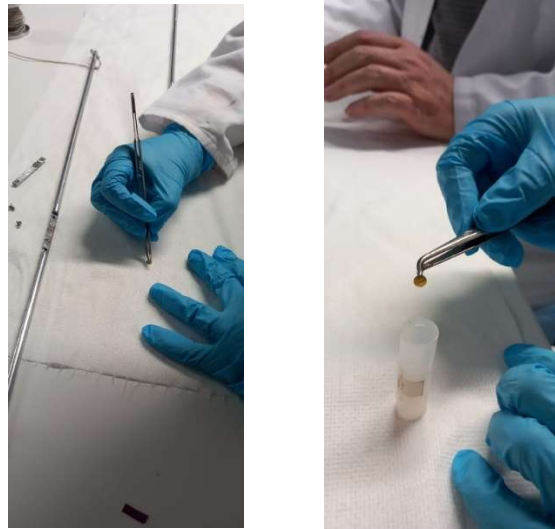


Figure 8. Flattening irradiated gold foils (left) and grouping them according to radial location (right)

To obtain accurate neutron flux measurements, the counter's plateau is first determined along with its background levels to ensure counts consistency. Activities are then measured via the counter and flux is calculated using the designated equation.

Internal air within the counter is vented to maintain methane gas purity. A stable voltage plateau is crucial for ionization. The detection setup includes a dual-counter system, preamplifier, interface, and computing hardware.



Figure 9. Measuring activity of irradiated foils using $4\pi\beta$ counter

4. Results and Discussion

Activity measurements, acquired as described earlier, are incorporated into the complete thermal flux equation (26). Table 2 presents the thermal neutron flux results for both covered and uncovered foils, with their distribution further visualized in Figure 8.

Table 2. Thermal neutron flux results

Distance from the core (cm)	T1 (min)	T2 (min)	Activity (Uncovered) (counts/sec)	Activity (Cd-covered) (counts/sec)	Neutron flux (neutron.cm ⁻² .s ⁻¹)
5.3	10	82	181.4	64	133427566.7
10.6	10	89	179.1	55.53	125753219.3
13.5	10	95	126.7	49.34	93182802.83
18.5	10	102	85.34	34.61	55872014.13
21.3	10	107	72.15	23.65	56166272.53

The measured neutron flux distribution aligns well with the Bessel function, the theoretical model for a bare, homogeneous reactor. The slight flux increase at the reactor's periphery is due to the graphite reflector in the TRIGA reactor, which scatters and reflects escaping neutrons back into the core. This confirms both the TRIGA reactor's efficacy and the reliability of our measurement methodology. The flux shape, visible in Figure 10, closely resembles the theoretical curve shown in Figure 1.

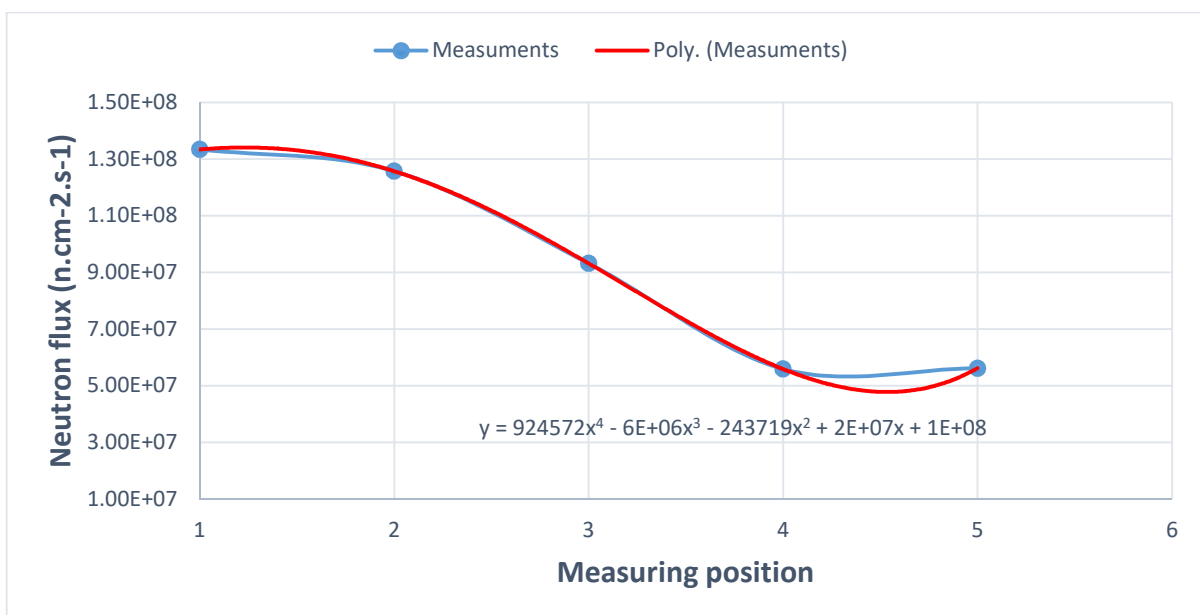


Figure 10. Radial distribution of neutron flux density in TRIGA reactor

5. Conclusion

Neutron flux measurement is an important parameter for nuclear research, and this study validates the utility of the gold foil activation method in performing such measurements. Experimental results were adjusted for Cd-correction, temperature dependency and self-shielding effects, offering a detailed thermal neutron flux profile at varying core distances. Comparison between theoretical and experimental flux shape showed good qualitative agreement. This work serves as both an educational resource and a template for experimental research, outlining each experimental step clearly as well as the reason behind it.

Future work may explore alternative materials for flux measurement and further optimize the gold foil activation method for specific reactor configurations, as was done here at the TRIGA reactor in Vienna.

- 6. ACKNOWLEDGMENT.** This work was done within the 2023 Safeguards Traineeship Programme organized by the International Atomic Energy Agency (IAEA) and at Atominstytut (TU Wien). Special thanks to Dr. Mario Villa, Dr. Andreas Musilek (TU Wien) and Dr. Susan E. Pickett, Dr. Haori Yang (IAEA) [Neutron Flux Measurement in the TRIGA Reactor using Gold Foil Activation Method].

References

- [1] International Atomic Energy Agency (1982), *Dosimetry for criticality accidents: A Manual*.
- [2] Borio di Tigliole, A., Cammi, A., Chiesa, D., Clemenza, M., Manera, S., Nastasi, M., Pattavina, L., Ponciroli, R., Pozzi, S., Prata, M., Previtali, E., Salvini, A., & Sisti, M. (2014). Triga reactor absolute neutron flux measurement using activated isotopes. *Progress in Nuclear Energy*, 70, 249–255. <https://doi.org/10.1016/j.pnucene.2013.10.001>
- [3] Safeguards Traineeship, Practical exercises in research reactors, March 1 – April 1, 2023, Vienna, Austria.
- [4] K. H. Beckurts and K. Wirt (1972), *Neutron physics*.
- [5] International Atomic Energy Agency (1987), *Handbook on Nuclear Activation Data, Technical reports series 273*, Vienna, 1987.
- [6] [Core \(tpub.com\)](https://tpub.com)
- [7] [File:Au-198-decay-scheme.svg - Wikimedia Commons](#)
- [8] Glasstone, S., & Edlund, M. C. (1957). *The elements of nuclear reactor theory*. Van Nostrand.

- [9] Sathian, D., Chougaoonkar, M. P., & Mayya, Y. S. (2010). A new technique for beta attenuation studies in neutron activation foils using 4π - coincidence system. *Radiation Protection Dosimetry*, 142(2–4), 92–98. <https://doi.org/10.1093/rpd/ncq261>
- [10] Berthold Technologies Beta counter manual.
- [11] Mueck, K., & Bensch, F. (1973). Cadmium correction factors of several thermal neutron foil detectors. *Journal of Nuclear Energy*, 27(9), 677–688. [https://doi.org/10.1016/0022-3107\(73\)90025-7](https://doi.org/10.1016/0022-3107(73)90025-7)
- [12] Borio di Tigliole, A., Cammi, A., Chiesa, D., Clemenza, M., Manera, S., Nastasi, M., Pattavina, L., Ponciroli, R., Pozzi, S., Prata, M., Previtali, E., Salvini, A., & Sisti, M. (2014). Triga reactor absolute neutron flux measurement using activated isotopes. *Progress in Nuclear Energy*, 70, 249–255. <https://doi.org/10.1016/j.pnucene.2013.10.001>
- [13] Als-Nielsen, J. (1967). Corrections in the gold foil activation method for determination of neutron beam density. *Nuclear Instruments and Methods*, 50(2), 191–196. [https://doi.org/10.1016/0029-554x\(67\)90040-7](https://doi.org/10.1016/0029-554x(67)90040-7)
- [14] Knoll, G. F. (2000). Radiation detection and measurement. John Wiley & Sons, Inc.

ნეიტრონების ნაკადის გაზომვა ოქროს ფოლგის აქტივაციის მეთოდის გამოყენებით TRIGA-ს ტიპის ბირთვულ რეაქტორში

თორნიკე ქიმერიძე^{1,2}; თრან ჩან ჰაი ნგუენ³

¹სსიპ - დავით აღმაშენებლის სახელობის საქართველოს ეროვნული თავდაცვის აკადემია

²სსიპ - სოხუმის ილია ვეკუას ფიზიკა-ტექნიკის ინსტიტუტი

³დალატის ბირთვული კვლევის ინსტიტუტი, დალატი, ვიეტნამი

რეზიუმე

ნეიტრონები ნაკადის გაზომვა ბირთვული ფიზიკის განუყოფელი ნაწილია, რომელიც განსაკუთრებით მნიშვნელოვანი პარამეტრია ბირთვული რეაქტორების უსაფრთხო მუშაობისათვის და ასევე, დიდ გავლენას ახდენს შემდეგ მიმართულებებზე: ბირთვული ინჟინერია, სამედიცინო ფიზიკა და მასალათმცოდნეობა. წინამდებარე ნაშრომში წარმოდგენილი კვლევა დეტალურად აღწერს ნეიტრონების ნაკადის სქემას ვენის ატომური ინსტიტუტის TRIGA რეაქტორში, სადაც იყენებენ ოქროს ფოლგის ნიმუშებს ნეიტრონების ნაკადის განსაზღვრისათვის. აღნიშნული პროცესი დაფუძნებულია სამიზნე ნიმუშების აქტივაციის მეთოდზე და შემდგომ მათ გაზომვაზე. აქედან გამომდინარე, მომზადდა იდენტური ოქროს ფოლგის ნიმუშები, რომელიც 10 წუთის განმავლობაში სხივდებოდა რეაქტორის ბირთვში და შემდგომ შეფასდა 4π დეტექტორის გამოყენებით.

ნეიტრონების ნაკადის განაწილება თეორიულად იყო მოდელირებული, როგორც ბესელის ფუნქცია და ჯვარედინი მიმართულების საწინააღმდეგოდ განხორციელდა სამიზნე ნიმუშების განლაგება და შემდგომ მათი აქტივაციის გაზომვა, რათა ექსპერიმენტულად მიგველო თერმული ნეიტრონების ნაკადის სქემა. დასკვნები ცხადყოფს თეორიულ და ექსპერიმენტულ მონაცემებს შორის ახლო კავშირს მიუხედავად იმისა, რომ ბირთვული რეაქტორის გარე პერიფერიებზე ნეიტრონების ნაკადი უმნიშვნელოდ იმატებს, რაგდან მის ირგვლივ განლაგებულ გრაფიტის ბლოკებს აქვს თვისება თერმული ნეიტრონებს არეკვლის. ეს ნაშრომი შეიცავს ღირებულ მონაცემებს ნეიტრონების ნაკადის განაწილების შესახებ TRIGA-ს ტიპის რეაქტორებში, რომელიც ფართოდ გამოიყენება რეაქტორების ექსპერიმენტებსა და ბირთვული რეაქტორის უსაფრთხო ოპერირებისათვის.

საკვანძო სიტყვები: ნეიტრონების ნაკადი, აქტივაციის ანალიზი; ექსპერიმენტული ბირთვული ფიზიკა; რეაქტორების ფიზიკა.